NJC

New Journal of Chemistry

An international journal of the chemical sciences

www.rsc.org/njc

Volume 34 | Number 7 | July 2010 | Pages 1225–1492

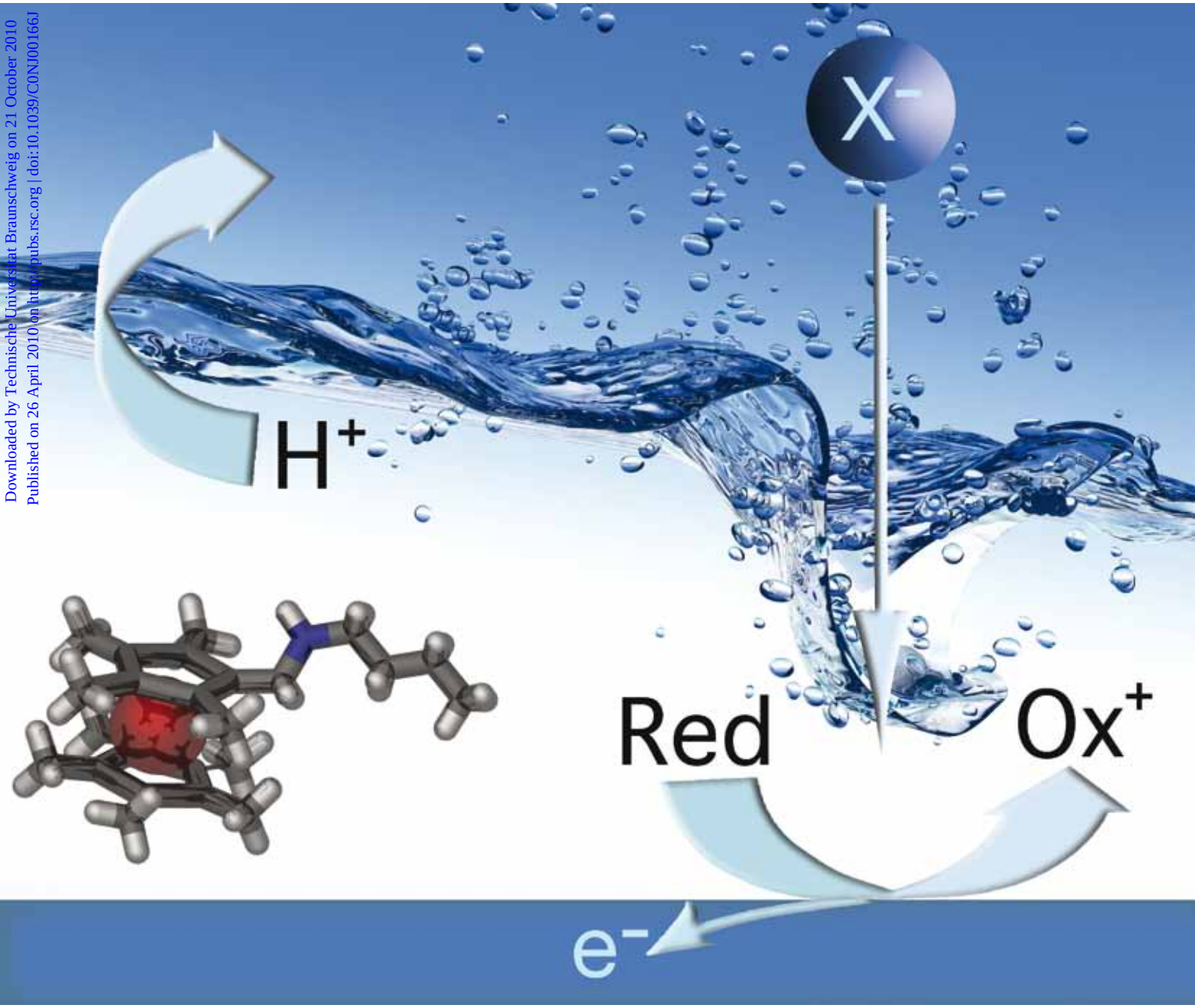

ISSN 1144-0546

RSC Publishing

PAPER

Tony D. James and Frank Marken *et al.*
A permethylated ferrocene redox system

1144-0546(2010)34:7;1-L

N,*N*-Butyl-decamethylferrocenyl-amine reactivity at liquid | liquid interfaces: electrochemically driven anion transfer *vs*. pH driven proton transfer

Andrew M. Kelly, Najoua Katif, Tony D. James* and Frank Marken*

Received (in Victoria, Australia) 2nd March 2010, Accepted 11th March 2010
First published as an Advance Article on the web 26th April 2010
DOI: 10.1039/c0nj00166j

We have developed a permethylated ferrocene redox system with a butylamine substituent for application in liquid | liquid ion sensors. The steric hindrance associated with the methyl groups results in an electrochemical system where the ferricenium derivative is chemically inert and the redox system remains chemically reversible, even for applications in aqueous or biphasic media. *N*,*N*-Butyl-decamethylferrocenyl-amine is soluble in hydrophobic organic solvents, such as 4-(3-phenylpropyl)pyridine (PPP) and *N*-octyl-pyrrolidone (NOP), and is employed here under "microphase" conditions, deposited in the form of microdroplets onto an electrode and immersed in aqueous buffer solutions. It is shown that under these conditions, electron transfer and proton transfer are only weakly coupled, and that anion transfer dominates the microphase redox process over the entire pH range. The corresponding biphasic Pourbaix diagram is discussed.

1. Introduction

There is a widespread need for novel moisture-stable redox tags, for example, in new types of bioelectrochemical sensors,[1] in redox active nanostructures[2] and for new redox systems for liquid | liquid ion transfer processes[3] with applications in ion-sensing devices. In aqueous or other highly polar media, the oxidized forms of many conventional ferrocenes are chemically unstable. The oxidation of ferrocene to the ferricenium cation is often associated with nucleophilic attack, the unwanted loss of cyclopentadienyl ligands, and the liberation of solvated Fe^{3+}.[4] Electronic stabilization can be achieved with more electron-donating ligands, but steric stabilization is more effective in preventing attack on the Fe^{3+}. By shielding the ferrocene redox system, for example with 10 methyl substituents, the resulting ferricenium derivative becomes much more inert towards nucleophilic attack and the redox system remains electrochemically reversible, even for applications in aqueous or in biphasic media.[5] However, the steric constraint of the methyl groups in decamethylferrocene leads to the need for more harsh synthetic conditions to enable effective covalent modification. In this study, a chemically robust decamethyl-ferrocenyl-amine derivative is synthesized and employed to explore reaction conditions in liquid | liquid systems. The organic phase contains the redox system and is present as a "microphase".

Microphase conditions in liquid | liquid electrochemical studies are beneficial[6] (i) by simplifying the experimental procedure[7] and (ii) by allowing simultaneous electron and ion transfer processes to occur in the same reaction zone.[8–10] Liquid | liquid microphase redox processes have been reported in microdroplets of water in immiscible organic liquids immobilized on graphite electrode surfaces[11] or on specifically-designed porous surfaces.[12,13] The schematic drawing in Fig. 1 indicates the coupling of electron transfer and interfacial anion or proton transfer required to maintain charge neutrality. The size of the microdroplet or microphase should be small (*ca.* 1 μm) to minimize effects from transport and resistance in the organic phase. Typical redox systems that have been employed in this type of experiment are n-butylferrocene,[14] decamethyl-ferrocene,[15] porphyrinato complexes[16] and phenylenediamine derivatives.[17]

Herein, we report the facile formation of nonamethyl-ferrocene-carboxaldehyde and its condensation with butylamine to give novel redox-active imine and amine derivatives. The resulting chemically robust decamethylferrocenyl redox systems are investigated by voltammetry in acetonitrile and by ion-transfer voltammetry under microphase conditions as a function of pH. Both anion and proton transfer processes are observed and explained based on a biphasic Pourbaix diagram.

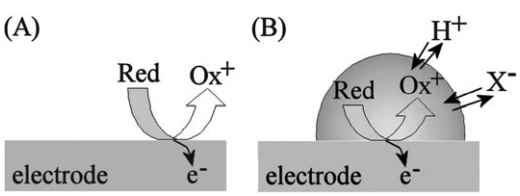

Fig. 1 Schematic drawing of (A) a redox process in a single liquid phase, and (B) a redox process in an organic microphase immersed in an aqueous solution and in contact with an electrode.

Department of Chemistry, University of Bath, Bath, BA2 7AY, UK. E-mail: t.d.james@bath.ac.uk, f.marken@bath.ac.uk

2. Experimental

2.1 Reagents

All commercial reagents and solvents were purchased from Sigma-Aldrich Company Ltd. and Fischer Scientific UK, and were used without further purification, unless otherwise mentioned. Argon (BOC) was employed to de-aerate solutions, and experiments were conducted at 20 ± 2 °C.

2.2 Instrumentation

Analytical thin layer chromatography (TLC) was performed on pre-coated silica gel 60 F_{254} plates. Visualization on TLC was achieved by the use of a UV light (254 nm). Flash column chromatography was undertaken on silica gel (60 F_{254} 400–630 mesh). Infrared spectra were recorded on a Perkin-Elmer Spectrum RX spectrometer between 4400 and 450 cm^{-1}. Samples were either evaporated from $CHCl_3$ on an NaCl disc (neat) or mixed with KBr in a mortar and pressed into a disc (KBr). All vibrations (n) are given in cm^{-1}. Nuclear magnetic resonance spectra were run in $CDCl_3$ on a Brüker Avance 300 instrument. ^1H NMR spectra were recorded at 300.22 MHz and {1H}–^{13}C NMR spectra at 75.50 MHz. Chemical shifts are expressed in parts per million and are reported relative to the residual solvent peak or to tetramethylsilane as an internal standard. The multiplicities and general assignments of the spectroscopic data are denoted as: singlet (s), doublet (d), triplet (t), quartet (q), unresolved multiplet (m) and broad (br). Coupling constants are expressed in Hz. Mass spectra were acquired using a micrOTOFQ electrospray time-of-flight (ESI-TOF) mass spectrometer (Bruker Daltonik GmbH) at the University of Bath. The micrOTOFQ spectrometer was coupled to an Agilent Technologies 1200 LC system. 10 μL of sample was directly injected into the mass spectrometer. Nitrogen was used as the nebulising gas and was applied at a pressure of 1 bar. Nitrogen was also used as a drying agent, supplied at a flow rate of 8 L min^{-1} and a temperature of 110 °C. Capillary melting points were recorded using a Büchi 535 melting point apparatus. Readings were taken from a mercury-in-glass thermometer and are reported uncorrected at the meniscus point. Where the sample changed colour or evolved gas during or after the melt, thermal decomposition (dec) is noted.

Electrochemical data were recorded on a microAutolab III instrument (Ecochemie, NL) employing a 4.9 mm diameter basal plane pyrolytic graphite electrode (Le Carbon UK Ltd.), a platinum wire counter electrode and a saturated calomel (SCE) reference electrode.

2.3 Procedures

2.3.1 Synthesis of nonamethylferrocenecarboxaldehyde. Decamethylferrocene (5.00 g, 15.32 mmol) was added to a stirred solution of pre-ground barium manganate (pestle and mortar; 19.63 g, 76.61 mmol) in 1 : 1 benzene : Et_2O (40 mL) and placed in an ultrasound bath for 10 min. Then the mixture was heated to 45 °C for 18 h before being allowed to cool to room temperature and the barium residues removed by suction filtration. The solvent was then evaporated under reduced pressure and the crude product purified by silica gel chromatography (Et_2O : hexane 1 : 50) to afford the desired product as a pale red solid (3.30 g, 63%); R_f (Et_2O : hexane 3 : 10) 0.14; m.p. 196–199 °C (dec); ν_{max} (solid)/cm^{-1} 1661 (C=O); δ_H (300 MHz; $CDCl_3$): 9.90 (1H, s, C*H*O), 1.91 (6H, s, C(C*Me*)$_2$(CHO)), 1.70 (6H, s, C(CHO)C(C*Me*)$_2$)) and 1.58 (15H, s, C(C*Me*)$_5$); δ_C (75 MHz; $CDCl_3$): 196.1, 86.4, 83.2, 81.0, 73.0, 9.7 and 9.4; HRMS (ESI^+) found 340.1409 ($[M]^+$; $C_{20}H_{28}FeO$ requires 340.1484).

2.3.2 Synthesis of *N,N*-butyl-decamethylferrocenyl-imine. Nonamethylferrocenecarboxaldehyde (50 mg, 0.15 mmol) was heated to reflux in a solution of butylamine (15 mL, 152 mmol) for 18 h before being allowed to cool to room temperature and the butylamine removed under reduced pressure to afford the title compound as a deep orange oil (59 mg, 100%); ν_{max} (film)/cm^{-1} 1635 (C=N); δ_H (300 MHz; $CDCl_3$): 8.08 (1H, s, C*H*N), 3.38 (2H, t, J = 7.0 Hz, CH_2N), 1.88 (6H, s, C(C*Me*)$_2$(CHN)), 1.66 (6H, s, C(CHN)C(C*Me*)$_2$)), 1.60 (17H, m, C(C*Me*)$_5$ and CH_2CH$_2$N) 1.50–1.41 (2H, m, CH_2CH$_3$) and 0.89 (3H, t, J = 8.0 Hz, CH_3CH$_2$); δ_C (75 MHz; $CDCl_3$): 161.8, 82.9, 81.1, 80.1, 74.3, 63.4, 34.2, 21.1, 14.4, 10.4, 9.9 and 9.5; HRMS (ESI^+) found 395.2405 ($[M]^+$; $C_{24}H_{37}FeN$ requires 395.2348).

2.3.3 Synthesis of *N,N*-butyl-decamethylferrocenyl-amine. Lithium aluminium hydride powder (24 mg, 0.63 mmol) was carefully added to a stirred solution of *N,N*-butyl-decamethyl-ferrocenyl-imine (50 mg, 0.13 mmol) in dry THF (15 mL) under an argon atmosphere. The mixture was then heated to reflux for 18 h before being allowed to cool to room temperature. Benzene (10 mL), EtOAc (5 mL, dropwise), and 5 M NaOH (a few drops) were added until the precipitation of insoluble material was complete. The mixture was filtered, the residue washed with benzene : methanol (80 : 20, 20 mL) and the filtrate evaporated under reduced pressure. Dichloromethane was added and the solution filtered a second time before removal of the solvent *in vacuo* afforded the title compound as a yellow oil. (43 mg, 83%); ν_{max} (film)/cm^{-1} 2962 (s), 2901 (s), 1427 (s) and 1374 (s); δ_H (300 MHz; $CDCl_3$): 3.62 (1H, br s, N*H*), 2.71 (2H, br s, C(CMe)$_2$(CH_2N)), 2.58 (2H, t, J = 7.4 Hz, CH$_2$CH_2N), 1.95–1.07 (31H, m, C(CH$_2$N)C(C*Me*)$_2$, C(CH$_2$N)C(*Me*)$_2$, C(C*Me*)$_5$ and CH_2CH_2CH$_3$) and 0.81 (3H, m, CH_3CH$_2$); δ_C (75 MHz; $CDCl_3$): 81.5, 80.1, 72.3, 46.4, 44.0, 28.7, 20.6, 14.0, 10.5, 10.1 and 9.9; HRMS (ESI^+) found 397.2500 ($[M]^+$; $C_{24}H_{39}FeN$ requires 397.2426).

3. Theory

Processes in microphase environments are of interest in emulsion and immobilized microdroplet cases where the liquid | liquid interface is dominating the reactivity and transport into the organic phase can (at least in a first approximation) be neglected. For redox active molecule B with Brønsted base character, the following equilibria can be formulated by taking into account the associated liquid | liquid anion transfer processes to maintain charge neutrality. The one-electron oxidation of B (associated with interfacial anion transfer) is defined by eqn (1) (effects due to non-ideality are neglected).

$B(org) + X^-(aq) \rightleftarrows B^+(org) + X^-(org) + e^-$ with

$$E_{B^+/B} = E^0_{B^+/B} + \Theta_{X^-} + \frac{RT}{F}\ln\frac{[B^+]}{[B]} \quad (1)$$

In this expression, all terms describing the anion transfer are summarized into

$$\Theta_{X^-} = \Theta^0 + \tfrac{RT}{F}\ln\frac{[X^-(org)]}{[X^-(aq)]}$$

where Θ^0 denotes the standard liquid | liquid interfacial transfer potential.[18] The corresponding one-electron oxidation of protonated species BH^+ is defined in eqn (2).

$BH^+(org) + X^-(aq) \rightleftarrows BH^{2+}(org) + X^-(org) + e^-$ with

$$E_{BH^{2+}/BH^+} = E^0_{BH^{2+}/BH^+} + \Theta_{X^-} + \frac{RT}{F}\ln\frac{[BH^{2+}]}{[BH^+]} \quad (2)$$

The corresponding acid/base equilibria with associated anion transfer across the liquid | liquid interface are defined in eqn (3) and eqn (4).

$BH^+(org) + X^-(org) \rightleftarrows B(org) + H^+(aq) + X^-(aq)$ with

$$K_B = \frac{[B]\times[H^+]}{[BH^+]}\times\frac{[X^-(aq)]}{[X^-(org)]} \quad (3)$$

$BH^{2+}(org) + X^-(org) \rightleftarrows B^+(org) + H^+(aq) + X^-(aq)$ with

$$K_{B^+} = \frac{[B^+]\times[H^+]}{[BH^{2+}]}\times\frac{[X^-(aq)]}{[X^-(org)]} \quad (4)$$

Zone I: When the pH value of the aqueous phase is sufficiently acidic, a simple one-electron transfer at the triple phase boundary will be associated with anion transfer from the aqueous into the organic phase. There is no associated proton transfer. The midpoint potential observed in cyclic voltammograms, $E_{mid,I} = \frac{1}{2}(E_p^{ox} + E_p^{red})$, can be derived approximately[19] from the Nernst expression in eqn (2) (see eqn (5)).

$$E_{mid,I} = E^0_{BH^{2+}/BH^+} + \Theta^0 + \frac{RT}{F}\ln\frac{3c_0}{2} - \frac{RT}{F}\ln[X^-(aq)] \quad (5)$$

Midpoint potential $E_{mid,I}$ is pH-independent but does depend on (i) the concentration of the transferring anion in the aqueous phase and in the organic phase, and (ii) the total concentration of the redox system in the organic phase, c_0.

Zone III: A similar expression based on eqn (1) applies for the case of sufficiently alkaline conditions (see eqn (6)). Again, a pH-independent midpoint potential is predicted.

$$E_{mid,III} = E^0_{B^+/B} + \Theta^0 + \frac{RT}{F}\ln\frac{c_0}{2} - \frac{RT}{F}\ln[X^-(aq)] \quad (6)$$

Zone II: At a pH value close to the pK_{B^+} value, the oxidation of the protonated BH^+ is expected to yield B^+. The process is accompanied by the transfer of a proton from the organic into the aqueous phase, and there is no anion involvement. Substitution of eqn (4) into eqn (2) gives the corresponding expression for $E_{mid,II}$ (see eqn (7)).

$$E_{mid,II} = E^0_{BH^{2+}/BH^+} + \Theta^0 - \frac{RT}{F}\ln K_{B^+} + \frac{RT}{F}\ln[H^+(aq)] \quad (7)$$

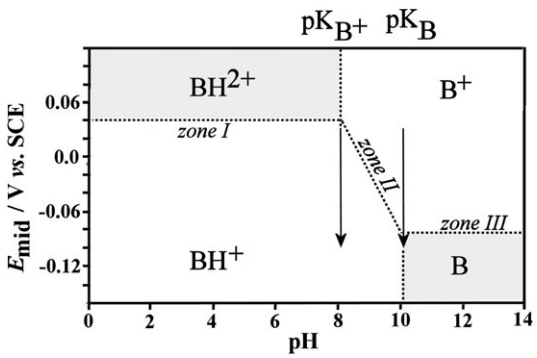

Fig. 2 A schematic drawing (biphasic Pourbaix diagram) explaining the effects of pH and applied potential on the major species in an organic microphase–aqueous electrolyte two-phase redox system (see text).

By equating $E_{mid,I}$ and $E_{mid,II}$, the point of intersection is obtained at

$$pH_{I,II} = pK_{B^+} - \log\frac{3c_0}{2[X^-(aq)]}$$

The concentration of the organic redox system is usually similar to the concentration of the aqueous anion so that in good approximation $pH_{I,II} \approx pK_{B^+}$. Similarly, at the intersection point between zone II and zone III

$$pH_{I,II} = pK_{B^+} - \log\frac{c_0}{2[X^-(aq)]}$$

and therefore in good approximation $pH_{II,III} \approx pK_B$. The predicted redox behaviour for the liquid | liquid microphase system is summarized in the biphasic Pourbaix diagram[20] in Fig. 2.

4. Results and discussion

The synthesis of nonamethylferrocene aldehyde from decamethylferrocene with $BaMnO_4$ was reported previously in 2001 by Stankovic *et al.*[21] and in 1984 by Kreiblin *et al.*[22] Power ultrasound was reported to improve the yield of the mono-aldehyde. Here, only a short burst of ultrasound was employed to break up and disperse the oxidizing agent prior to mild heating in a 1 : 1 benzene : Et_2O solution (see Fig. 3).

After work-up, an isolated yield of 63% nonamethylferrocene aldehyde **2** was obtained, with the parent decamethyl-

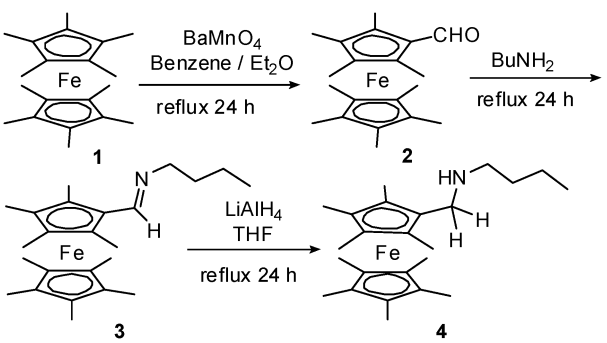

Fig. 3 A reaction scheme summarizing the conversion of decamethylferrocene (**1**) to imine **3** and amine **4** derivatives.

Table 1 Summary of voltammetric data (scan rate 0.01 V s^{-1}) for the oxidation and re-reduction of 2 mM decamethylferrocene derivatives **1–4** in acetonitrile (0.1 M NBu_4PF_6) obtained at a 4.9 mm diameter basal plane pyrolytic graphite electrode

	E_p^{ox}/V *vs.* SCE	E_p^{red}/V *vs.* SCE	ΔE_p/mV	E_{mid}/V *vs.* SCE
1	−0.056	−0.155	99	−0.105
2	0.365	0.199	166	0.282
3	0.092	−0.003	95	0.045
4	0.014	−0.087	101	0.036

ferrocene being recovered in 13% yield. Mono-aldehyde **2** was reacted further by heating to reflux with butylamine as the solvent to give butylimine derivative **3** in quantitative yield after a simple evaporation of the excess butylamine *in vacuo*. In the presence of moisture, this imine derivative readily hydrolyzed back to aldehyde **2**, and therefore amine derivative **4** was synthesized by reduction with lithium aluminium hydride. The conversion was carried out in THF under reflux to afford amine derivative **4** in 83% yield. All decamethylferrocene derivatives were studied by conventional solution voltammetry and by ion transfer voltammetry. The electrochemical properties of decamethylferrocene derivatives **1–4** were first studied in acetonitrile solution with 0.1 M NBu_4PF_6 electrolyte. For all derivatives, a well-defined voltammetric oxidation process occurred with a characteristic shift in the midpoint potential, defined here as $E_{mid} = \frac{1}{2}(E_p^{ox} + E_p^{red})$, consistent with the electron withdrawing nature of the aldehyde **2** > imine **3** > amine **4** > methyl **1** functional groups (see Table 1). The peak-to-peak separation suggests some sluggishness in the rate of electron transfer and/or uncompensated resistance in the organic solution phase.

Next, cyclic voltammograms were recorded under biphasic conditions[23] with the ferrocene derivative dissolved into an organic water-immiscible solvent (either NOP = *N*-octylpyrrolidone or PPP = 4-(3-phenylpropyl)-pyridine) and immobilized onto the basal plane of a pyrolytic graphite electrode surface in the form of microdroplets. The aqueous phase contained 0.1 M KPF_6 electrolyte salt and this allowed PF_6^- anion transfer from the aqueous into the organic solution phase during oxidation. In the case of amine derivative **4**, it was realized that protonation of the amine would occur as a function of pH in the aqueous phase, and therefore experiments were conducted with pH control in the presence of 10 mM phosphate buffer. Fig. 4A–C show typical cyclic ion transfer voltammograms for PF_6^- transfer during the oxidation of the amine derivative, where the presence of two distinct oxidation/reduction processes—P1 and P2—indicate the presence of **4** and $\mathbf{4H}^+$, respectively. Based on these voltammetric responses, the mechanism for P1 and P2 could be identified (see eqn (8) and eqn (9)).

$$\mathbf{P1}: \mathbf{4}(org) + PF_6^-(aq) \rightleftarrows \mathbf{4}^+(org) + PF_6^-(org) + e^- \quad (8)$$

$$\mathbf{P2}: \mathbf{4H}^+(org) + PF_6^-(aq) \rightleftarrows \mathbf{4H}^{2+}(org) + PF_6^-(org) + e^- \quad (9)$$

The plot of the midpoint potential *vs.* pH (see Fig. 4D) is indicative of a switch from anion transfer (see zone I and zone III in Fig. 2) to proton transfer (see zone II in Fig. 2).

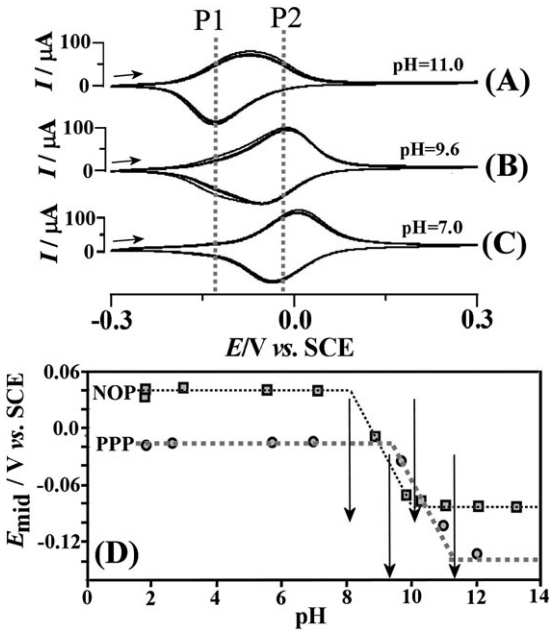

Fig. 4 Cyclic voltammograms (three cycles, scan rate 10 mV s^{-1}) for the oxidation and re-reduction of **4** and $\mathbf{4H}^+$ (*ca.* 200 mM in PPP deposited onto 4.9 mm diameter basal plane pyrolytic graphite) immersed in aqueous 0.1 M KPF_6 at pH (A) 11.0, (B) 9.6 and (C) 7.0. The plot in (D) shows the midpoint potential obtained in NOP and in PPP as a function of pH. Lines correspond to the characteristics predicted in the biphasic Pourbaix diagram (see Fig. 2). Acid/base constants are in NOP pK_{B+} = 8.1 and pK_B = 10.1, and in PPP pK_{B+} = 9.3 and pK_B = 11.3 in the presence of aqueous 0.1 M PF_6^-.

The fact that the midpoint potential in zone I and in zone III are only *ca.* 124 mV separated suggests that the protonation of the *N*,*N*-butyl-decamethylferrocenyl-amine has only a small electronic effect on the Fe(II/III) redox system. Correspondingly, the effect of the Fe(II/III) redox state on the acid–base characteristics is relatively minor, and this causes zone II to remain small. From the transition points in the Pourbaix diagram, the biphasic pK_A values can be estimated.

A plot of the midpoint potential for $\mathbf{4}/\mathbf{4H}^+$ oxidation as a function of pH (see Fig. 4D) reveals a solvent-dependent transition and distinct pK_A values in each solvent. In NOP, biphasic acid–base constants of pK_{B+} = 8.1 and pK_B = 10.1 are obtained, and in PPP pK_{B+} = 9.3 and pK_B = 11.3. Note that the midpoint potentials in zone I and III are dependent on the aqueous anion (on the type and concentration) and that these pK_A values are valid only for aqueous 0.1 M PF_6^-. However, based on the appropriate Nernst expression (see the Theory section), the shift in pK_A is predictable. In both solvents, the difference in midpoint potentials in zone I and III is approximately 124 mV, and correspondingly the difference in pK_{B+} and pK_B is approximately 2. It is interesting to note that the zone II lines for both solvents almost superimpose, which suggests that a difference in anion solvation in NOP and PPP is the dominating factor in determining the shift in pK_A (and not proton solvation or solvation effects involving the redox system). The same type of shift in midpoint potentials and pK_A values is predicted when the nature of

Table 2 A summary of voltammetric data (scan rate 10 mV s^{-1}) for the oxidation and re-reduction of 200 mM decamethylferrocene derivatives **1–4** in PPP or NOP deposited onto a 4.9 mm diameter basal plane pyrolytic graphite electrode and immersed into aqueous 0.1 M KPF_6

	PPP			NOP		
	E_p^{ox}/V *vs.* SCE	E_p^{red}/V *vs.* SCE	E_{mid}/V *vs.* SCE	E_p^{ox}/V *vs.* SCE	E_p^{red}/V *vs.* SCE	E_{mid}/V *vs.* SCE
1	−0.139	−0.215	−0.177	−0.091	−0.248	−0.169
2	0.162	0.108	0.135	0.212	0.079	0.145
3	−0.013	−0.015	−0.014	0.052	0.000	0.026
4	−0.123	−0.153	−0.138	−0.063	−0.105	−0.084
$\mathbf{4H^+}$	0.021	−0.039	−0.014	0.059	0.021	0.040

the aqueous electrolyte anion is made more hydrophilic or more hydrophobic.

The comparison of ion transfer voltammetric data for the ferrocene derivatives (see Table 2) shows similar trends in NOP and PPP solvent media. Due to the electron withdrawing substituents on the ferrocene, the shift in midpoint potentials is aldehyde **2** > imine **3** ≈ ammonium $\mathbf{4H^+}$ > amine **4** > methyl **1** functional groups. However, only *N*,*N*-butyl-decamethylferrocenyl-amine **4** gives stable and well-defined voltammetric responses due to its inert and hydrophobic characteristics.

5. Conclusion

New and chemically robust decamethylferrocenyl-amine derivatives have been synthesized. In particular, amine derivative **4** (and similar derivatives) will be of interest as a readily available redox label and as a novel redox system for biphasic electrochemical processes. The butylamine functional group can be substituted for other amines and the sterically-shielded ferrocene introduced as a versatile redox building block. The protonation of the amine functional group is dependent on the redox state of the ferrocene, and solvent/anion dependent biphasic pK_A values have been obtained. These biphasic pK_A values are best understood as anion-dependent "aqueous" pK_A values. In order to convert these biphasic pK_A data into organic solvent-specific pK_A data, the aqueous/organic proton transfer equilibrium has to be taken into account. Typical pK_A values in organic solvents (*e.g.* for acetonitrile) are *ca.* 16 units more positive.[24]

Acknowledgements

We would like to thank the Leverhulme Trust (F/00351/R) for their financial support. N. K. thanks the Analytical Division of the Royal Society of Chemistry for an Analytical Studentship stipend.

References

1 P. M. Levine, P. Gong, R. Levicky and K. L. Shepard, *Biosens. Bioelectron.*, 2009, **24**, 1995.
2 O. Buriez, E. Labbe, P. Pigeon, G. Jaouen and C. Amatore, *J. Electroanal. Chem.*, 2008, **619–620**, 169.
3 C. E. Banks, T. J. Davies, R. G. Evans, G. Hignett, A. J. Wain, N. S. Lawrence, J. D. Wadhawan, F. Marken and R. G. Compton, *Phys. Chem. Chem. Phys.*, 2003, **5**, 4053.
4 R. Prins, A. R. Korswage and A. G. Kortbeek, *J. Organomet. Chem.*, 1972, **39**, 335.
5 Š. Komorsky-Lovrić, K. Riedl, R. Gulaboski, V. Mirceski and F. Scholz, *Langmuir*, 2002, **18**, 8000.
6 T. Kakiuchi, *Anal. Chem.*, 1996, **68**, 3658.
7 F. Marken, R. D. Webster, S. D. Bull and S. G. Davies, *J. Electroanal. Chem.*, 1997, **437**, 209.
8 F. Marken, R. G. Compton, C. H. Goeting, J. S. Foord, S. D. Bull and S. G. Davies, *Electroanalysis*, 1998, **10**, 821.
9 U. Schröder, R. G. Compton, F. Marken, S. D. Bull, S. G. Davies and S. Gilmour, *J. Phys. Chem.*, 2001, **105**, 1344.
10 N. Katif, R. A. Harries, A. M. Kelly, J. S. Fossey, T. D. James and F. Marken, *J. Solid State Electrochem.*, 2009, **13**, 1475.
11 M. J. Bonné, C. Reynolds, S. Yates, G. Shul, J. Niedziolka, M. Opallo and F. Marken, *New J. Chem.*, 2006, **30**, 327.
12 D. Rayner, N. Fietkau, I. Streeter, F. Marken, B. R. Buckley, P. C. B. Page, J. del Campo, R. Mas, F. X. Munoz and R. G. Compton, *J. Phys. Chem. C*, 2007, **111**, 9992.
13 M. A. Ghanem and F. Marken, *Electrochem. Commun.*, 2005, **7**, 1333.
14 J. D. Wadhawan, R. G. Evans and R. G. Compton, *J. Electroanal. Chem.*, 2002, **533**, 71.
15 V. Mirceski, R. Gulaboski and F. Scholz, *J. Electroanal. Chem.*, 2004, **566**, 351.
16 S. M. MacDonald, M. Opallo, A. Klamt, F. Eckert and F. Marken, *Phys. Chem. Chem. Phys.*, 2008, **10**, 3925.
17 M. Opallo, M. Saczek-Maj, G. Shul, C. M. Hayman, P. C. B. Page and F. Marken, *Electrochim. Acta*, 2005, **50**, 1711.
18 F. Scholz, U. Schröder and R. Gulaboski, *Electrochemistry of Immobilized Particles and Droplets*, Springer, Berlin, 2005, pp. 213.
19 F. Scholz and R. Gulaboski, *ChemPhysChem*, 2005, **6**, 16.
20 M. Pourbaix, *Atlas of Electrochemical Equilibria in Aqueous Solutions*, Pergamon, Houston Texas, 1966.
21 E. Stankovic, S. Toma, R. Van Boxel, I. Asselberghs and A. Persoons, *J. Organomet. Chem.*, 2001, **637–639**, 426.
22 A. Z. Kreiblin, M. I. Rybinskya and S. S. Fabeeva, *Izv. Akad. Nauk. Ser. Khim.*, 1984, 362.
23 F. Marken, K. J. McKenzie, G. Shul and M. Opallo, *Faraday Discuss.*, 2005, **129**, 219.
24 N. Isaacs, *Physical Organic Chemistry*, Longman, London, 1996, pp. 238.